Measurement of the Concentration of Mn^{2+} and Mn^{3+} in the Manganese-Catalyzed 1,4-Cyclohexanedione−Acid−Bromate Reaction Using Redox-Triggered Magnetic Resonance Spectroscopy

Melanie M. Britton[†]

Magnetic Resonance Research Centre, Department of Chemical Engineering, University of Cambridge, New Museums Site, Pembroke Street, Cambridge CB2 3RA, U.K., and School of Chemistry, University of Birmingham, Edgbaston, Birmingham B15 2TT, U.K.

Received: August 11, 2006; In Final Form: September 29, 2006

A new nuclear magnetic resonance (NMR) experiment is reported, where the spectrometer is triggered using the output from a combination redox electrode. This technique was used to probe redox oscillations in the 1,4-cyclohexanedione−acid−bromate reaction. Manganese(III) acetate or manganese(II) sulfate was used as the catalyst, and the periodic change in concentration of Mn^{2+}/Mn^{3+} ions was determined as a function of redox potential. The concentration of Mn^{3+} ions was at a maximum at high redox potential and at a minimum at low redox potential. Also, redox potentials were found to not be dominated by the Mn^{2+}/Mn^{3+} couple.

Introduction

Nuclear magnetic resonance (NMR) spectroscopy has proved to be a valuable technique used in the study of oscillating reactions, such as the Belousov−Zhabotinsky (BZ),[1,2] 1,4-cyclohexanedione−acid−bromate (CHD)[3] and Bray−Liebhafsky (BL)[4] reactions. By acquiring ^{1}H NMR spectra, it has been possible to identify reaction products and intermediates. By following their change in concentration over time, it has been possible to measure rate constants[5] and test reaction mechanisms.[3,6]

Observation of organic reactants and products frequently requires the suppression of the dominant water signal, allowing these more dilute species to be detected. However, the solvent water signal can also be used, to probe oscillations produced by these reactions. Proton (^{1}H) NMR spin−lattice (T_1) and spin−spin (T_2) relaxation times and the chemical shift of water molecules are affected by the presence and concentration of paramagnetic species. Schlüter and Weiss[2] showed in the manganese-catalyzed BZ reaction that the T_1 of the water signal was sensitive to the oscillatory change in oxidative state of the manganese ion catalyst. By using NMR titration (NMRT),[2] where the signal intensity of the water peak changes as a function of T_1, they were able to monitor oscillations. Later Hansen and Ruoff[1] also showed, in a similar system, that the chemical shift and the T_2 relaxation time of the water peak could also be used to monitor periodic interconversion between Mn^{2+} and Mn^{3+}. Finally, Stanisavljev et al.[4] observed that the chemical shift of water molecules in the Bray−Liebhafsky reaction could be used to follow oscillations. However, they found that changes in chemical shift and line width were not as smoothly periodic as in the BZ reaction and suggested that this was a reflection of the complexity of behavior of the system. A detailed mechanism has not yet been established for this reaction and the origin of these chemical shift oscillations is less clear than in the BZ reaction; however, it is believed that periodic changes in oxygen concentration, which is paramagnetic, are responsible.

In experiments used to follow the kinetics of organic molecules, it is possible to accumulate multiple scans during the reaction, and so monitor the gradual increase or decrease of these molecules. By accumulating multiple scans, it is possible to increase the signal-to-noise ratio[7] and to also enable the use of water suppression sequences,[3] which frequently require phase cycling and hence multiple scans. However, in NMR experiments used to probe oscillations, single-scan experiments must be used, ensuring the duration of the experiment is significantly shorter that the oscillatory period, so allowing several experiments to be performed per oscillation. Measurements of T_2 relaxation times and chemical shift employ simple pulse-acquire pulse sequences. The chemical shift of the water signal can be directly measured from the spectrum and its T_2 comes from the full-width at half-height (fwhm) of the peak.[7] It should be noted that using the line width gives a value for T_2^* rather than T_2,[7] so a Lorentzian (or Gaussian) line shape is required and the sample needs to be well shimmed. In NMRT experiments measuring T_1, a 180° inversion pulse is applied prior to the excitation-pulse and acquisition. The delay τ between the inversion and excitation pulses is typically set so that a null point is produced. At the null point ($\tau_{null} = T_1 \ln 2$) the signal intensity is zero. T_1 changes are then probed by changes in the signal intensity.

While these experiments have proved successful in directly observing oscillations, which can then be compared with oscillations in redox potential, they have not been able to directly connect the change in potential with the change in oxidative state of the catalyst. This paper reports a new technique, which is able to directly measure the catalyst concentration at a given point in the redox cycle. Previously, measurement of relaxation times has been used to directly measure catalyst concentrations.[8] By combining this method with control of the spectrometer, data can be acquired at a particular point within a redox oscillation, coupling the measurement of catalyst concentration with redox potential and so better understand the link between the two. The technique is particularly useful in the CHD reaction, where the redox potential in the uncatalyzed system is believed to be determined by the couple between 1,4-

[†] E-mail: m.m.britton@bham.ac.uk.

10.1021/jp065197h CCC: $33.50
Published on Web 11/11/2006

hydroquinone (H_2Q) and its product 1,4-benzoquinone (Q), and the influence of a metal ion catalyst, when present, is less well understood. This paper reports the first experiments, which synchronize the NMR spectrometer with the oscillations in redox potential and so *trigger* NMR measurements at specified points within the oscillating redox potential. These *redox-triggered* NMR experiments enable data to be acquired at controlled and specified points in an oscillation and hence enable multiple scans to be acquired. Using this technique, it is possible to directly link the change in oxidative state of the metal ion catalyst, through measurement of T_2 relaxation times, with the redox oscillations. Redox-triggered CPMG[9] measurements are presented, which probe oscillations in the manganese-catalyzed CHD reaction.

Theory

There is a simple linear relationship between the overall relaxation rate ($1/T_2$) of a solution containing paramagnetic species (x) and the concentration of that species, [x], as shown in

$$\frac{1}{T_2} = k_x[x] + \frac{1}{T_{2_{sol}}} \quad (1)$$

$1/T_{2_{sol}}$ is the diamagnetic contribution from the solvent nuclei to the relaxation rate and k_x is the *relaxivity* of the paramagnetic species. If the relaxivity of the paramagnetic ion is known, then its concentration can be calculated from the relaxation rate of the solution. Where there is more than one paramagnetic species, as is the case in the Mn-catalyzed CHD reaction, the relaxation rate becomes a sum of contributions from both paramagnetic species and the solvent

$$\frac{1}{T_2} = \frac{1}{T_{2_{ox}}} + \frac{1}{T_{2_{red}}} + \frac{1}{T_{2_{sol}}} \quad (2)$$

where ox and red would represent the oxidized (Mn^{3+}) and reduced (Mn^{2+}) states of the manganese catalyst, which are both paramagnetic. So, by measuring the relaxivity of both the oxidized and reduced ions and knowing the total concentration of ions (e.g., $[Mn]_0 = [Mn_{ox.}] + [Mn_{red.}]$), it becomes possible to calculate the concentration of either ion from a measured T_2 relaxation time.[8]

Experimental Section

CHD Reaction. The reacting solution was 2.5 M H_2SO_4 (Aldrich), 0.1 M 1,4-cyclohexanedione (Aldrich), 0.1 M $NaBrO_3$ (Fluka) and 2.5×10^{-4} manganese(III) acetate (Aldrich) or manganese(II) sulfate (BDH). All reactants were used without further purification. Solutions were prepared in distilled, deionized water.

NMR Relaxation Measurements. For an introduction to the principles of magnetic resonance, the reader is referred elsewhere.[7] The NMR spectrometer used was a Bruker Biospin DMX-300, with a 7.0 T superconducting magnet, operating at a proton resonance frequency of 300 MHz, equipped with shielded and water-cooled gradient coils. All NMR experiments were done at a temperature of 21 ± 0.2 °C, using a 25 mm radio frequency coil. NMR data was analyzed using the software package PROSPA.[10]

Relaxation experiments were performed to measure the transverse, T_2, relaxation times of solutions containing oxidized (Mn^{3+}) and reduced (Mn^{2+}) states of the transition metal ion complex using both manganese(III) acetate and manganese(II) sulfate. In the case of manganese acetate, Mn^{3+} solutions were produced by dissolving manganese(III) acetate in 2.5 M sulfuric acid and the reduced solution was produced by adding 0.1 M 1,4-cyclohexanedione (CHD). In the case of the manganese sulfate solutions, Mn^{2+} solutions were produced by dissolving manganese(II) sulfate in 2.5 M sulfuric acid and the oxidized solution was produced by adding bromate.

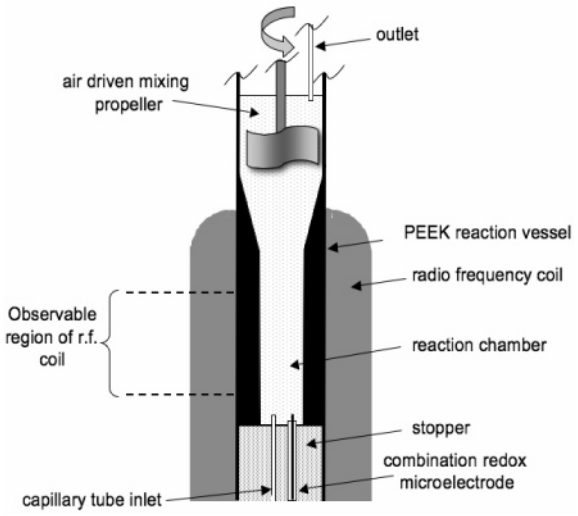

Figure 1. Schematic diagram for reaction vessel inside the NMR gradient coils and magnet. The mixing propeller is driven from the top of the magnet using compressed air. The inlet tube and lead for the microelectrode are fed upward from the bottom of the magnet and the outlet tube is fed out of the magnet from the top. The volume of the reaction vessel was 20 cm^3. The inner diameter of the radio frequency coil was 25 cm, and the inner diameter of the reaction vessel was 10 mm.

Carr−Purcell−Meiboom−Gill (CPMG) experiments[7] were used to measure the T_2 relaxation times for the solutions at different concentrations. Typically, 128 echoes were collected, with an echo spacing of 2 ms, producing an echo train of duration 256 ms. Two signal averages were acquired with a repetition time of 1 s and the duration of an experiment was 2 s.

Apparatus. A reaction vessel was constructed in the NMR (Figure 1), which allowed the rapid or continuous injection of reactants. It was possible to run the device in batch mode or as a continuous stirred tank reactor (CSTR). The mixture was stirred in the vessel using an air driven mixing propeller, with a drive shaft that came down the length of the magnet bore. The mixing propeller was positioned above the detectable region of the radio frequency (rf) coil, so that the homogeneity of the static magnetic field ($\mathbf{B}_0$) was not adversely affected. Inside the reaction vessel there was a Pt combination microelectrode (Microelectrodes), reference type Ag/AgCl, which measured the redox potentials inside the NMR magnet. This was also placed just outside the observable region of the rf coil. Data from the electrode was recorded on a computer, through an RS232 interface, using Labview software (National Instruments).

Redox Trigger Device. A device was designed and manufactured that could trigger the NMR spectrometer to start an experiment at a specified redox potential, by generating a TTL signal. While the TTL signal was on, the spectrometer would run experiments. The potential used to trigger the spectrometer was chosen once the reaction started to oscillate and corresponded to a value either at the top or bottom of an oscillation. A command was inserted into the NMR pulse programs, which

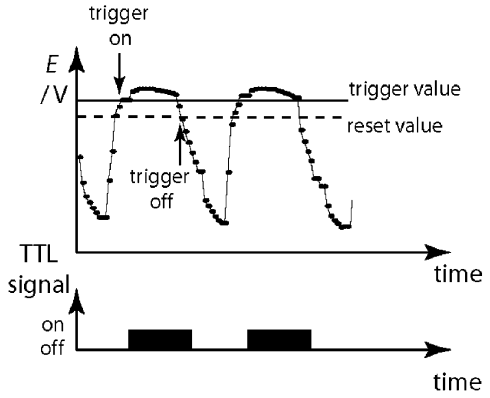

Figure 2. Plot of redox potential against time during oscillations in the 1,4-cyclohexanedione−acid−bromate reaction. The trigger and reset values, used for controlling the NMR spectrometer, are indicated on the plot. The associated TTL signal, sent to the spectrometer, is indicated below. The TTL signal is on once the redox potential is greater than the trigger value and is off once the redox potential falls below the reset value.

made the spectrometer wait for the TTL signal before starting the pulse sequence.

When triggering at the top of an oscillation, the TTL signal was on once the electrode potential reached the set value and above. The TTL signal only then stopped once the potential fell to a level approximately 30 mV below the trigger value. Similarly, if the spectrometer was to be triggered at the bottom of an oscillation, the TTL signal was sent once the electrode potential reached the set value and below. The TTL signal was only then stopped once the potential was 30 mV above the set value.

As the spectrometer would continue to run experiments while the TTL signal was being sent, care needed to be taken so that the spectrometer was triggered only once during an oscillation and always at the same point. Figure 2 shows a series of redox oscillations, with two lines marking the potential values when the TTL signal is on, and hence triggering the spectrometer, and when the device would reset, and hence the TTL signal switched off. In this example, triggering is at the top of the oscillation. As a CPMG experiment with 2 signal averages will take approximately 2 s, it is possible for this experiment to complete and even another one to start during the period the TTL pulse is sent. However, these experiments would then occur at different points during the oscillation, at points where the chemistry of the system was different, and it would not be possible to trace exactly when they occurred. Of course, this would not be desirable; therefore, it was important to ensure not only that another scan did not start during this period but also that the instrument was ready to trigger immediately when the TTL signal was sent for the following oscillation. This was done by setting a repetition time (typically 3−10 s) just longer than the period over which the TTL pulse was on, and the time depended on the periodicity of the oscillations. The chemistry of the system was then probed by inserting a delay after the trigger, so that the spectrometer collected data at all points within a redox cycle.

Results

The relaxivities of Mn^{3+} and Mn^{2+} ions were found from solutions of manganese acetate by plotting relaxation rate ($1/T_2$) against concentration for both oxidized (Mn^{3+}) and reduced (Mn^{2+}) solutions. Each slope was fitted[1] to a straight line (Figure 3a) as shown in

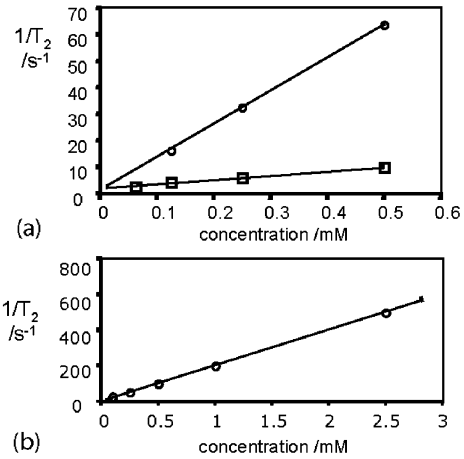

Figure 3. (a) Plot of relaxation rate ($1/T_2$) against concentration for manganese(III) acetate (□) and manganese(II) acetate (○). (b) Plot of relaxation rate ($1/T_2$) against concentration for manganese(II) sulfate.

$$\frac{1}{T_{2_{\text{Mn(II) acetate}}}} = 126.7 \times 10^3[\text{Mn}^{2+}] + 0.44 \qquad (3a)$$

$$\frac{1}{T_{2_{\text{Mn(III) acetate}}}} = 16.3 \times 10^3[\text{Mn}^{3+}] + 1.62 \qquad (3b)$$

$[Mn^{2+}]$ and $[Mn^{3+}]$ are the concentrations of the oxidized and reduced solutions, respectively, in M, and $1/T_{2_{\text{Mn(II) acetate}}}$; $1/T_{2_{\text{Mn(III) acetate}}}$ are the corresponding solvent molecule relaxation rates, in s^{-1}. The constant in each fit is the diamagnetic contribution to the relaxation rate from the solvent molecules. As the total concentration of manganese ions remains constant ($[Mn]_0$) it is possible to combine eqs 3a,b to produce expressions giving the concentration of reduced or oxidized ions for an observed relaxation rate

$$\frac{1}{T_{2_{\text{obs}}}} = 16.3 \times 10^3[\text{Mn acetate}]_0 + 110.4 \times 10^3[\text{Mn}^{2+}] + 1.02 \qquad (4a)$$

$$\frac{1}{T_{2_{\text{obs}}}} = 126.7 \times 10^3[\text{Mn acetate}]_0 - 110.4 \times 10^3[\text{Mn}^{3+}] + 1.02 \qquad (4b)$$

In these equations an average for the diamagnetic contribution from the solvent molecules has been used.

The same was done for manganese sulfate solutions. However, only a straight line for the Mn^{2+} solutions could be produced (Figure 3b) and the fit is

$$\frac{1}{T_{2_{\text{Mn(II) sulfate}}}} = 199.4 \times 10^3[\text{Mn}^{2+}] + 2.8 \qquad (5)$$

The Mn^{3+} solutions did not produce a straight line for a plot of concentration against relaxation rate. The reason for this is that bromate does not fully oxidize Mn^{2+}, as can been seen from reaction step R1 (Table 1), which is strongly reversible. Following the addition of bromate, a mixture of both oxidized and reduced ions is produced. As the concentration of manganese increases, so does the relative proportion of Mn^{2+} and

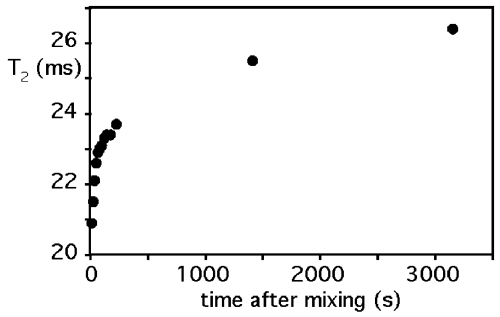

Figure 4. Plot of T_2 relaxation time against time during the reaction between 0.1 M bromate and manganese(II) sulfate in 2.25 M sulfuric acid.

TABLE 1: Reaction Steps Involved in Reaction between Acidic Bromate and Manganese

R1	$Br^- + HOBr + H^+ \leftrightarrow Br_2 + H_2O$
R2	$Br^- + HBrO_2 + H^+ \leftrightarrow 2HOBr$
R3	$Br^- + BrO_3^- + 2H^+ \leftrightarrow HOBr + HBrO_2$
R4	$2BrO_3^- + 2H^+ \leftrightarrow HBrO_2 + HBrO_4$
R5	$2HBrO_2 \rightarrow BrO_3^- + HOBr + H^+$
R6	$HBrO_2 + BrO_3^- + H^+ \leftrightarrow Br_2O_4 + H_2O$
R7	$Br_2O_4 \leftrightarrow 2BrO_2^\bullet$
R8	$Mn^{2+} + BrO_2^\bullet + H^+ \leftrightarrow Mn^{3+} + HBrO_2$

TABLE 2: Rate Constants for the Reaction Steps Involved in Reaction between Acidic Bromate and Manganese

	$k_{forward}$	$k_{reverse}$	ref
R1	8×10^9 mol^{-2} dm^6 s^{-1}	80 s^{-1}	14
R2	2.5×10^6 mol^{-2} dm^6 s^{-1}	2×10^{-5} mol^{-1} dm^3 s^{-1}	14
R3	1.2 mol^{-3} dm^9 s^{-1}	3.2 mol^{-2} dm^6 s^{-1}	14
R4	7×10^{-7} mol^{-1} dm^3 s^{-1}		18
R5	3×10^3 mol^{-1} dm^3 s^{-1}	$1 \times 10-^8$ mol^{-2} dm^6 s^{-1}	19
R6	48 mol^{-2} dm^6 s^{-1}	3.2×10^3 s^{-1}	14
R7	7.5×10^4 s^{-1}	1.4×10^9 mol^{-1} dm^3 s^{-1}	14
R8	8.5×10^4 mol^{-2} dm^6 s^{-1}	7.7×10^4 mol^{-1} dm^3 s^{-1}	14

Mn^{3+} ions. The line is therefore not linear and its slope is enhanced by the presence of Mn^{2+} ions, which have a greater relaxivity than Mn^{3+} ions. Alternative oxidants to bromate were investigated, such as PbO_2, which had been used successfully to oxidize ferroin.[11] However erratic conversion was observed with PbO_2 and no other suitable oxidants were found. However, while the relaxivity of the Mn^{3+} ions, $k_{Mn(III)}$, could not be directly measured, it can be fitted by following the change in relaxation time during the reaction of Mn^{2+} with bromate. Figure 4 shows a typical plot of T_2 against time after the addition of BrO_3^- (to a concentration of 0.1 M) to a solution of 2.5×10^{-4} M $MnSO_4$ in 2.25 M sulfuric acid. Following the addition of bromate, Mn^{2+} ions are oxidized to Mn^{3+} and there is a corresponding reduction in relaxation time. An equilibrium is reached between the oxidized and reduced states, at which point the T_2 relaxation time levels off. The mechanism for this reaction has been extensively studied and the oxidation of Mn^{2+} with bromate was simulated using the reaction steps and rate constants in Tables 1 and 2, with the same reactant concentrations as the reaction. From this, the concentrations of both states were determined as a function of time. As the contribution to the relaxation time of this system is known for the diamagnetic solvent and the Mn^{2+} ions, it is possible to calculate the relaxivity of Mn^{3+} by using it as a fitting parameter for the simulated T_2 plot compared to the experimental data. Using this method a relaxivity of $(105.0 \pm 2) \times 10^3$ was obtained for the Mn^{3+} ion. A plot showing the experimental and simulated T_2 times during this reaction is given is Figure 5, along with a plot of the corresponding change in Mn^{2+} concentration.

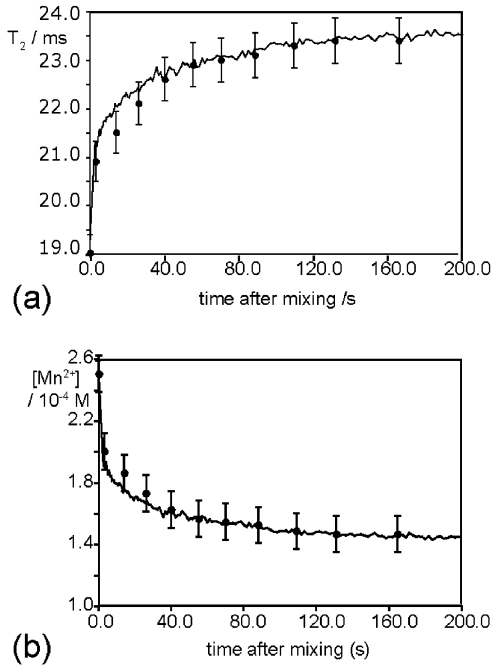

Figure 5. Experimental (●) and simulated (—) data of T_2 relaxation times (a) and Mn^{2+} concentration (b) against time during the reaction between 0.1 M bromate and manganese(II) sulfate in 2.25 M sulfuric acid.

Expressions giving the concentration of reduced or oxidized ions for an observed relaxation rate are

$$\frac{1}{T_{2_{obs}}} = 105.0 \times 10^3[\text{Mn sulfate}]_0 + 94.4 \times 10^3[Mn^{2+}] + 2.8 \quad (6a)$$

$$\frac{1}{T_{2_{obs}}} = 199.4 \times 10^3[\text{Mn sulfate}]_0 - 94.4 \times 10^3[Mn^{3+}] + 2.8 \quad (6b)$$

What can be seen from the relaxivities of the reduced and oxidized states is that the relaxivity of Mn^{2+} ions produced by dissolving manganese(II) sulfate is greater than for Mn^{2+} ions formed by manganese(III) acetate. The same is true for the oxidized ions also. This is most likely because manganese(II) sulfate forms a hexadentate aquo ion in solution, which has up to six coordinated water molecules surrounding it, while manganese(II) acetate will have less coordinated water molecules, due to the coordinated acetate molecules. As the number of coordinated water molecules is a factor in determining the relaxivity of a species[12] and the relaxivity tends to increase as the number of coordinated molecules increases, it is expected that manganese acetate would have a lower relaxivity, as is observed.

The complete conversion from Mn^{3+} and Mn^{2+} was also probed during the reaction between manganese(III) acetate (2.5×10^{-4} M) and 1,4-cyclohexanedione (0.01 M). Following the addition of CHD to a manganese(III) acetate solution, a series of T_2 measurements were taken. From the T_2 data the concentration of Mn^{2+} and Mn^{3+} could be calculated using their experimentally measured relaxivities (eqs 4a,b). These values were then compared with the concentrations from a simulation[13] of the reaction steps and rate constants in Tables 3 and 4. Figure 6 shows a plot of both experimental and simulated data for the change in concentration of Mn^{3+} during the reaction of CHD.

TABLE 3: Reaction Steps Involved in Reaction between CHD and Manganese[14]

R9	$2Mn^{3+} + CHD \rightarrow 2Mn^{2+} + H_2Q + 2H^+$
R10	$2Mn^{3+} + H_2Q \rightarrow 2Mn^{2+} + Q + 2H^+$

TABLE 4: Rate Constants for the Reaction Steps Involved in Reaction between CHD and Manganese

	$k_{forward}$, $mol^{-1}\ dm^3\ s^{-1}$	ref
R9	0.16	14
R10	1×10^3	14

There is excellent agreement between the experimental and simulated data. It is interesting to note that the rate constants for the two reactions involved were determined using $MnSO_4$[14] and there does not appear to be a difference in these values when manganese(III) acetate is used.

Finally, the interconversion between Mn^{2+} and Mn^{3+} was investigated during redox oscillations, for both manganese(II) sulfate or manganese(III) acetate catalysts. The spectrometer was triggered at the bottom of the redox oscillation for the manganese sulfate system and at the top for the manganese acetate system. A variable time delay was included in the pulse sequence, following the trigger command, so that it was possible to take measurements throughout the redox cycle. Figure 7 shows typical redox potential oscillations for both the manganese(II) sulfate or manganese(III) acetate catalyzed reactions. The amplitudes of these oscillations are the same for both systems. However, the periodicity is different, with the manganese(II) sulfate catalyzed reaction having a longer period. The origin of this was not investigated in this study.

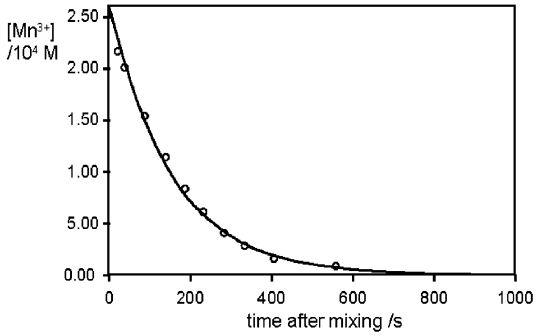

Figure 6. Experimental (●) and simulated (—) Mn^{3+} concentration during the reaction between 0.01 M 1,4-cyclohexanedione and 2.5×10^{-4} M manganese(III) acetate in 2.5 M sulfuric acid.

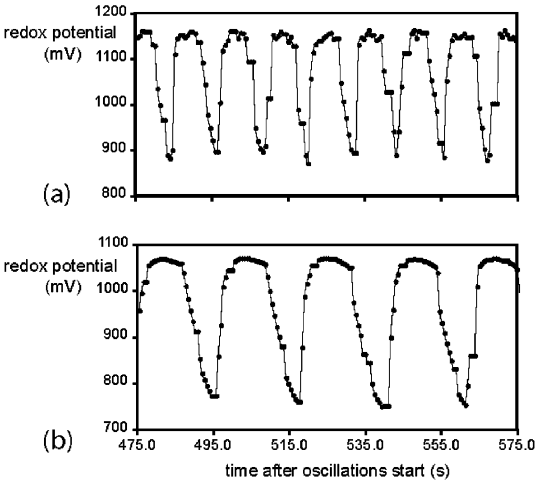

Figure 7. Measured redox potential for oscillations in the manganese acetate (a) and manganese sulfate (b) catalyzed CHD reaction. Initial reactant concentrations were [CHD] = 0.1 M, $[H_2SO_4]$ = 2.5 M, $[BrO_3^-]$ = 0.1 M, and [Mn] = 2.5×10^{-4} M.

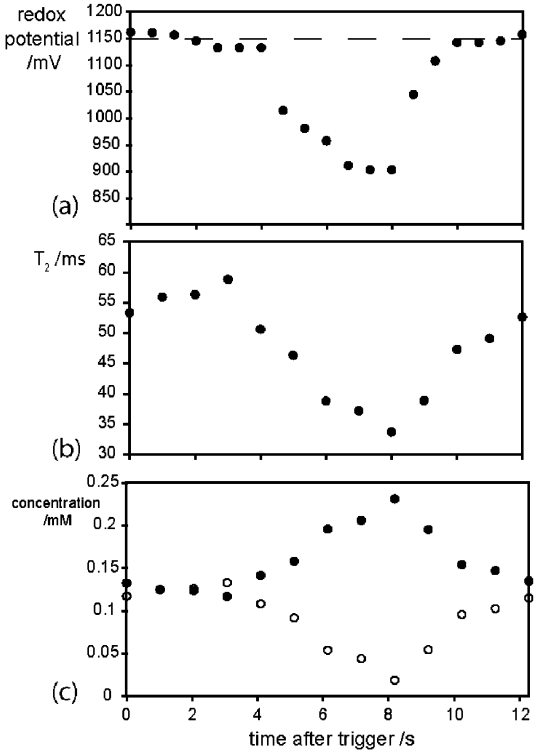

Figure 8. (a) Measured redox oscillation in a manganese acetate-catalyzed CHD reaction. (b) Redox-triggered T_2 measurement during redox oscillation. (c) Concentration of Mn^{2+} (●) and Mn^{3+} (○) during redox oscillation, determined from T_2 measurement. Initial reactant concentrations were [CHD] = 0.1 M, $[H_2SO_4]$ = 2.5 M, $[BrO_3^-]$ = 0.1 M, and [Mn] = 2.5×10^{-4} M.

Figures 7 and 8 display redox, T_2 relaxation time and concentration oscillations for the manganese(III) acetate and manganese(II) sulfate systems, respectively. Both systems show that a minimum T_2 is found at the lowest redox potential and a maximum T_2 is found at the highest redox potential. The redox potential reaches a maximum value and then remains there for a while before falling. Once this maximum value is reached, the T_2 is still increasing until its maximum is reached before the potential drops. Mn^{2+} is at a maximum when T_2 is lowest and a minimum when T_2 is highest. By comparing the redox and concentration plots, one can see that Mn^{2+} is at a maximum at the lowest point of the redox cycle and falls to a minimum as the redox increases. Finally, as has been seen in spatial patterns in this system,[8] there is not full conversion between Mn^{3+} and Mn^{2+}.

Discussion

For both systems, the minimum Mn^{2+} concentration (and hence maximum Mn^{3+} concentration) occurs before the redox starts to fall. This is more pronounced for the manganese sulfate system (Figure 9), which has a longer period. Here the maximum is almost in the middle of the high redox potential plateau. The Mn^{3+} concentration then starts to drop again immediately after its maximum, which is not matched in the redox potential, which remains high for a few seconds longer before also dropping. This suggests that the potential of the Pt electrode is not dominated by the Mn^{2+}/Mn^{3+} couple. Indeed, Szalai and coworkers suggested[15] that the redox potential of the Pt electrode, in the uncatalyzed reaction, was mainly dependent on the 1,4-hydroquinone (H_2Q)/1,4-benzoquinone (Q) couple. The results found in this work remain consistent with this. However, using this technique, it becomes possible for the first time to test this,

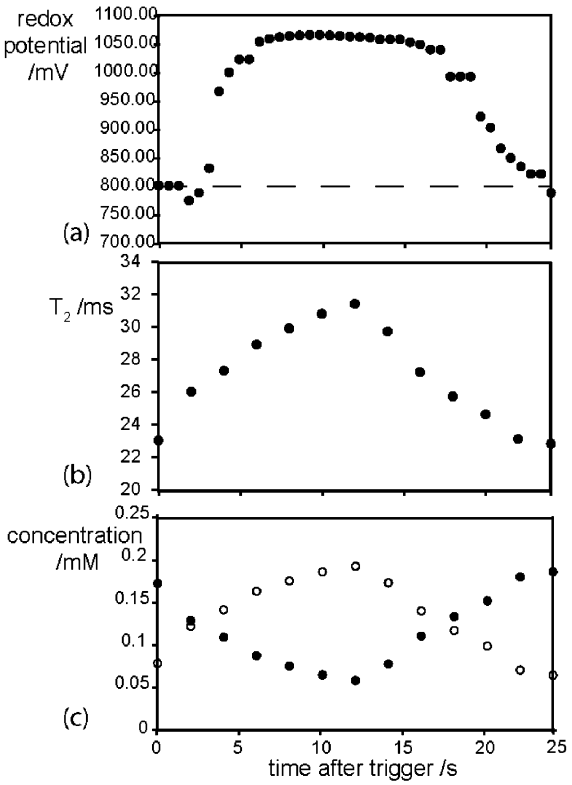

Figure 9. (a) Measured redox oscillation in a manganese sulfate-catalyzed CHD reaction. (b) Redox-triggered T_2 measurement during redox oscillation. (c) Concentration of Mn^{2+} (●) and Mn^{3+} (○) during redox oscillation, determined from T_2 measurement. Initial reactant concentrations were [CHD] = 0.1 M, [H_2SO_4] = 2.5 M, [BrO_3^-] = 0.1 M, and [Mn] = 2.5×10^{-4} M.

as the concentration of the hydroquinone can be followed during a redox cycle. This will require the use of a constantly fed stirred tank reactor (CSTR) to maintain the system in the oscillatory phase, allowing sufficient NMR experiments to be acquired to improve the signal-to-noise of the hydroquinone peak, which would be in dilute concentration (1×10^{-6} to 1.0×10^{-4} M).

Conclusions

This paper has presented the first direct measurement of metal ion catalyst concentration as a function of redox potential. By triggering the spectrometer at a specified point in the redox oscillation, the T_2 relaxation time, and hence concentration of Mn^{2+} or Mn^{3+}, can be directly linked. The scope of this technique, however, goes beyond linking redox potential with catalyst concentration and it allows a vast range of chemical processes, which are associated with changes in redox potential, to be probed. For example in the CHD reaction it has been suggested that the organic molecule 1,4-hydroquinone (H_2Q) underpins the oscillatory behavior of the system and the redox couple between it and its product 1,4-benzonquinone (Q), is believed to be responsible for potential oscillations in the CHD system. However, this key molecule has, as yet, not been directly observed. To demonstrate that this molecule is present and oscillates in synchronization with the potential oscillations, it is essential to be able to probe the system at controlled and specified points in the redox oscillation. Other possibilities include the ability to probe the periodic formation and disappearance of micelles during oscillations in the BZ reaction.[16] Also, it becomes possible to probe exchange pathways for processes that occur at specific redox potentials, ion concentration or pH using electrode- or pH-triggered NMR experiments, such as EXSY.[17] Equally, MR imaging experiments could also be triggered in this way.

Acknowledgment. M.M.B. thanks EPSRC for an Advanced Research Fellowship and Prof. Lynn F. Gladden and her group at the MRRC, Cambridge University, for support.

References and Notes

(1) Hansen, E. W.; Ruoff, P. *J. Phys. Chem.* **1989**, *93*, 264.
(2) Schlüter, A.; Weiss, A. *Ber. Bunsen-Ges. Phys. Chem.* **1981**, *85*, 306.
(3) Britton, M. M. *J. Phys. Chem. A* **2003**, *107*, 5033.
(4) Stanisavljev, D.; Begovic, N.; Zujovic, Z.; Vucelic, D.; Bacic, G. *J. Phys. Chem. A* **1998**, *102*, 6883.
(5) Hansen, E. W.; Ruoff, P. *J. Phys. Chem.* **1988**, *92*, 2641.
(6) Hansen, E. W.; Gran, H. C.; Ruoff, P. *J. Phys. Chem.* **1985**, *89*, 682.
(7) Callaghan, P. T. *Principles of Nuclear Magnetic Resonance Microscopy*; Oxford University Press: Oxford, U.K., 1991.
(8) Britton, M. M. *J. Phys. Chem. A* **2006**, *110*, 2579.
(9) Fukushima, E.; Roeder, S. B. W. *Experimental Pulse NMR: a Nuts and Bolts Approach*; Addison-Wesley: Reading, MA, 1981.
(10) Magtritek. Prospa; http://www.magritek.com/prospa.html, 2000.
(11) Szalai, I.; Kurin-Csorgei, K.; Orban, M. *Phys. Chem. Chem. Phys.* **2002**, *4*, 1271.
(12) Lauffer, R. B. *Chem. Rev.* **1987**, *87*, 901.
(13) Hinsberg, W. D.; Houle, F. A. Chemical Kinetics Simulator Program; 1.01 ed.; IBM Corporation, available at <http://www.almaden.ibm.com/st/msim>, 2000.
(14) Szalai, I.; Kurin-Csorgei, K.; Epstein, I. R.; Orban, M. *J. Phys. Chem. A* **2003**, *107*, 10074.
(15) Szalai, I.; Körös, E. *J. Phys. Chem. A* **1998**, *102*, 6892.
(16) Yoshimoto, M.; Shirahama, H.; Kurosawa, S.; Naito, M. *J. Chem. Phys.* **2004**, *120*, 7067.
(17) Jeener, J.; Meier, B. H.; Machmann, P.; Ernst, R. R. *J. Chem. Phys.* **1979**, *71*, 4546.
(18) Gao, Y.; Försterling, H.-D. *J. Phys. Chem.* **1995**, *99*, 8638.
(19) Field, R. J.; Forsterling, H. D. *J. Phys. Chem.* **1986**, *90*, 5400.